



Stochastic Assessment of Predictions and Uncertainties for Reflectance Losses Based on Experimental Data for Three Australian Sites

Giovanni Picotti¹, Huy Truong Ba¹ , Cody B. Anderson^{1,2} , Michael E. Cholette¹, Theodore A. Steinberg¹, and Bruce Leslie³

¹ Queensland University of Technology, Australia

² Politecnico di Milano, Italy

³ Vast, Australia

*Correspondence: Giovanni Picotti, g.picotti@qut.edu.au

Abstract. A stochastic reflectance loss model is applied to extended datasets of experimental data collected at three sites in Australia, each representative of a different environment: urban, rural, and remote outback. The three sites are analysed in terms of TSP (Total Suspended Particles) or PM10 (Particulate Matter below 10µm in diameter), depending on the available dust sampler deployed at each location. Assessment of seasonal and daily patterns are also performed for further understanding of local phenomena likely to affect soiling in the area. Airborne dust concentration data are exploited to provide density distributions of expected daily reflectance losses. These mean losses for the three sites are 0.31 pp/day, 0.72 pp/day, and 0.77pp/day for the outback, rural, and urban location, respectively. These values and their distributions are paramount for evaluation of a prospective plant profitability, planning for operating plants cleaning scheduling, and assessment of a prospective CSP location at site selection phase. The developed methodology is capable of providing highly valuable information based on easily measurable airborne dust concentration data only, hence becoming a critical step for de-risking CSP plants financing and deployment.

Keywords: Reflectance, Predictions, Stochastic, Uncertainties, Experiments

1. Introduction

The soiling of solar collectors and the induced loss of efficiency is a paramount issue in CSP. The reduction of heliostats reflection directly diminishes the thermal input available for power generation [1] and varies dramatically depending on site location and weather characteristics, which is further affected by seasonality [2]. Currently, artificial cleaning is the most widespread technique employed to mitigate the detrimental effects of heliostats soiling [2], [3]. However, cleaning is expensive and in most cases requires significant amount of water that may be scarce in CSP-favorable locations. The impact of the combined cost for cleaning and electricity generation losses due to soiling on a CSP plant profit could be as high as 20% in dusty areas [4]. Furthermore, the inherently inhomogeneous nature of soiling in a solar field implies potentially unbalanced thermal fluxes on central receiver systems, thus affecting their lifetime and required maintenance activities [5]. Predictive models and techniques have been developed to assess and predict soiling losses using a variety of methods, including physical-based models [6], regressions analyses [7], Artificial Neural Networks [8], [9], or on-site

measurements with hand-held reflectometers [10] and semi-automated devices [11], [12]. Statistical tools can be integrated with developed soiling models to obtain reliable assessments of the inherent uncertainty of the reflectance losses predictions. In this study, a stochastic approach developed and validated in a previous publication [13] is exploited to evaluate the impact of different uncertainty sources, to predict soiling losses on heliostats deployed in three different locations in Australia, and to assess the interval of confidence for long-term predictions. The soiling model is tuned for each site based on experimentally collected data over a few weekly experimental campaigns, and subsequently applied to predict long term soiling losses.

2. Stochastic Models

The analysis performed in this study is based on the *constant-mean* model described in a previous publication by some of the authors [13]. The key components and assumptions of the exploited model will be briefly described in this section to facilitate the understanding of the proposed methodology and guide the reader through the innovative application of the aforementioned modelling technique. The *constant-mean* model is the simpler version of the models proposed in [13], which is bereft of any dependency on environmental factors described in [6] except for the airborne dust concentration. The simplified model detailed in Section 2.1 was selected since it provides better predictions on novel data and has a simple structure amenable to prediction. Eventually, to estimate the statistical distribution of daily soiling losses, a Monte Carlo simulation is conducted, which is detailed in Section 2.2.

2.1 Reflectance Loss Model

The reflectance loss model provides estimates of the statistical distribution of daily soiling losses based on long-term experimental airborne dust data and short-term reflectance data measurements obtained on site. Its description is detailed below, summarizing from [13] and highlighting those aspects that are most relevant for the remainder of this paper.

The reflectance measurement r_k taken at time index k is modelled as

$$r_k = \rho(A_{soil,k}, \phi_k) + \epsilon_{r,k} \quad (1)$$

Where $\epsilon_{r,k} \sim \mathcal{N}(0, \sigma_{r,k}^2)$ varies with time, $A_{soil,k}$ is the projection area of the surface coverage due to soiling, and ϕ_k is the angle of incident of the measuring device. The measurement noise variance $\sigma_{r,k}^2$ is obtained computing the estimated variance of the mean of repeated measurements on the same reflective sample. The statistical distribution of the measured reflectance change between two consecutive time steps k and l is modelled as a normal distribution:

$$r_l - r_k \sim N(\mu_{l,k}, \sigma_{l,k}^2) \quad (2)$$

Where

$$\mu_{l,k} = -\tilde{\mu}b(\phi_k) \sum_{j=k}^{l-1} \alpha_j \cos(\theta_j) \quad (3)$$

$$\sigma_{l,k}^2 = \sigma_{dep}^2 b(\phi)^2 \sum_{j=k}^{l-1} \alpha_j^2 \cos^2(\theta_j) + \sigma_{r,k}^2 + \sigma_{r,l}^2 \quad (4)$$

Here, $b(\phi)$ is a function describing the effect of the incidence angle on the measurement, $\tilde{\mu}$ is a parameter describing the mean loss in one timestep, α is the ratio of measured airborne dust to that of some specified airborne dust distribution (usually from atmospheric literature based on the site characteristics [14]), and θ is the tilt angle of the mirror. Eventually, σ_{dep}^2 and $\sigma_{r,x}^2$ are parameters describing the uncertainty in the losses predictions and reflectance measurements, respectively. Since the time indices used above are arbitrary, this model can be used to estimate the statistical distribution of losses over any time interval, which is chosen as 1 day in this work.

For a more thorough and complete description of the reflectance loss model applied in this study, the interested reader is referred to a previous publications [13].

2.2 Monte Carlo Simulations

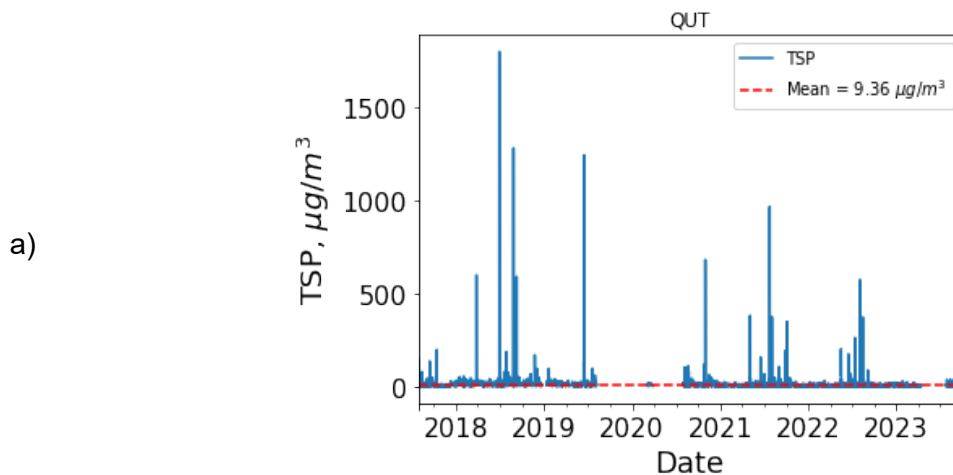
To estimate the statistical distribution of daily soiling losses, a Monte Carlo simulation is conducted by

- 1) Sampling the uncertain estimated model parameters;
- 2) Sampling the daily dust loadings from the long-term site airborne dust measurements;
- 3) Sampling the model's inherent uncertainty described by the normal distribution above (and the parameters sampled from 1) and 2)).

3. Experimental Sites Characterization

The three datasets are analysed to characterize each Australian experimental site in terms of airborne dust loading. The first dataset was collected in Brisbane and it is hence characteristic of an urban environment, the second site is located in Mount Isa, QLD, in a remote and desertic area isolated from anthropogenic sources, and the third one is located in the industrial area of the rural town of Wodonga, VIC. Furthermore, the properties of airborne dust in terms of seasonal and daily variation, as well as dust size distribution where possible, have been analysed in this study, based on large available datasets.

The measured airborne dust concentration for each of the three sites is represented in Figure 1, together with their mean value throughout the whole experimental period. The measurements for the QUT and Mount Isa sites are expressed in terms of TSP while those for Wodonga site are shown for PM10. This is due to the different dust sampler employed at each location. The sampler in Wodonga is also able to measure the cumulative airborne particle mass at five particle diameters (1, 2.5, 4, 10, 20 μm), providing further information that can be exploited for particle size distribution assessment.



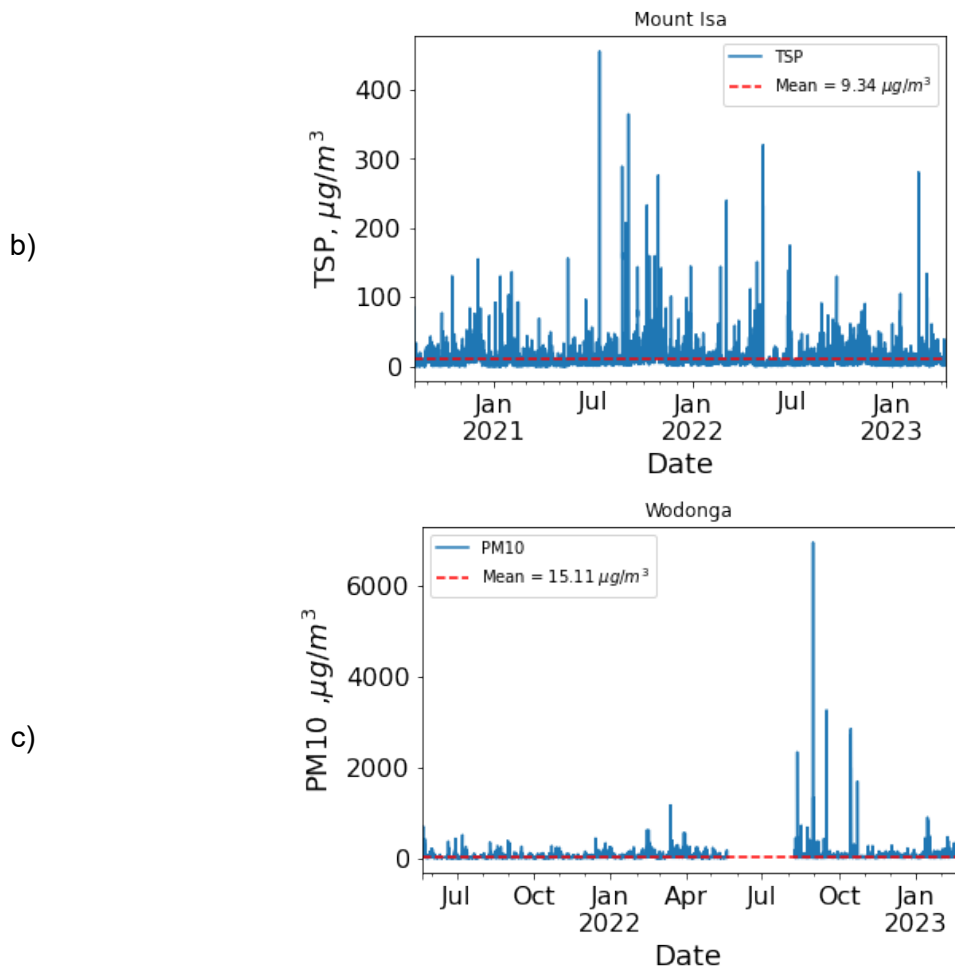


Figure 1. Airborne dust concentration for the three sites: a) Brisbane, b) Mount Isa, c) Wodonga

The data are also exploited to assess any observable seasonal or daily behaviour, that could further improve long-term soiling evaluations. Figure 2 provides a complete analysis of the TSP concentration measured at the QUT site. The monthly average over the last 5 years (2020 is missing due to malfunction of the device) suggests a moderate decrease of overall airborne dust mass concentration. However, the seasonal analysis represented in terms of difference from the overall mean, does not seem to suggest any significant variation throughout the year. The daily variation shows instead a higher peak in the early morning and a second lower peak in the evening, which could be explained by increased traffic in the neighbouring highway. The data shown for the Mount Isa site in Figure 3 (left) provides information regarding a moderate seasonality with higher dust loading in autumn (September to November in the Southern Hemisphere) and lower dust levels from summer to spring. This is partly explained by the more frequent rain occurrences during summer and spring, which have a scavenging effect on airborne particles. Figure 3 (right) shows instead the daily behaviour of airborne dust loading, which appears to have a maximum around 10am and decrease during the night. It may be explained by increased wind during the day that carries higher concentration of dust particles. Figure 4 (left) shows the monthly average PM_x for the site of Wodonga. Although there is limited data to infer anything conclusive regarding airborne dust concentration seasonality, the measurements collected so far suggest high particle concentrations in February, both for 2022 and 2023. Changes in airborne particle size distribution over the year can be assessed by analysing the difference between two PM_x measurements. For instance, the difference between PM₁ and PM_{2.5} provides the airborne mass concentration for particle diameters between 1 μm and 2.5 μm . Figure 4 (right) shows the intra-day synchronous average for each PM_x range. These figures show that particle sizes between 4 and 10 μm are the most significant contributor to airborne mass concentrations. The mass concentration for each

particle range shows evidence of anthropogenic pollution during the morning and afternoon, likely due to the nearby highway or manufacturing disturbances, with particle sizes between $2.5\mu\text{m}$ and $10\mu\text{m}$ showing the largest peaks near these times. Particles beyond these boundaries tend to not be affected at these peak time periods, suggesting that the particle size distribution may change throughout the day.

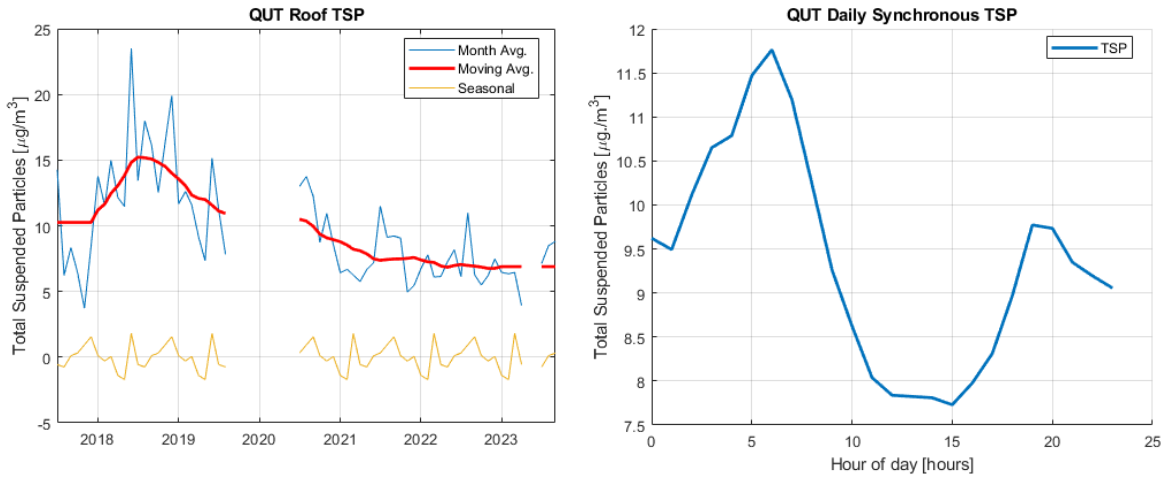


Figure 2. QUT TSP analysis

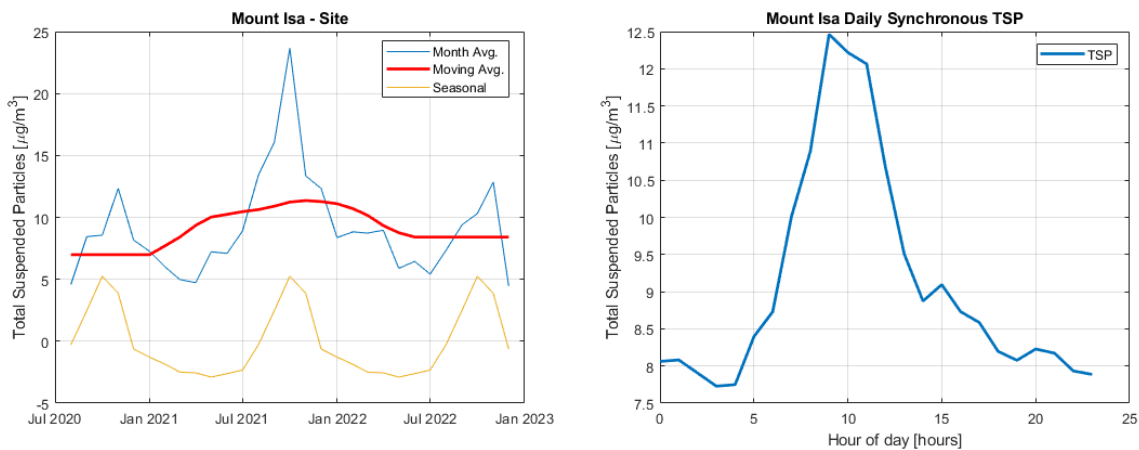


Figure 3. Mount Isa TSP analysis

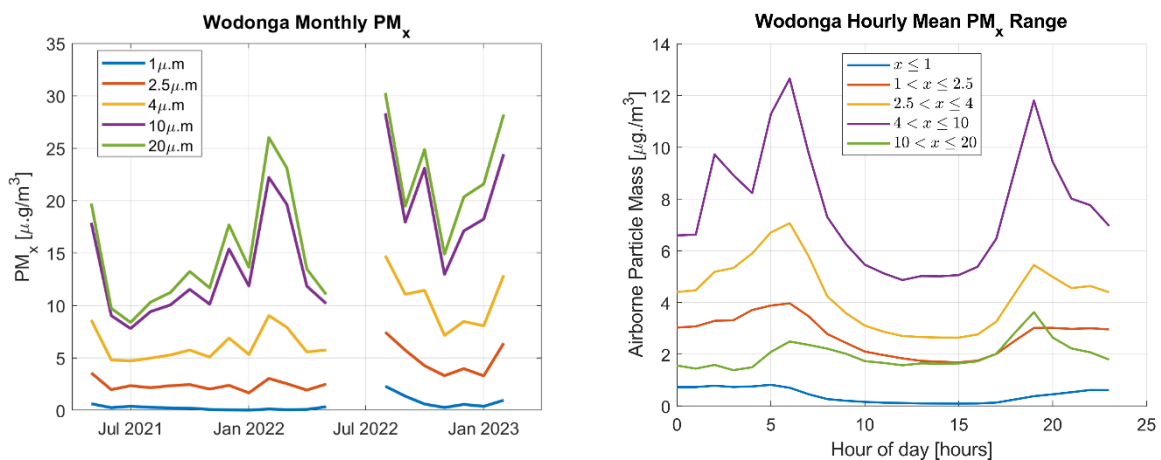
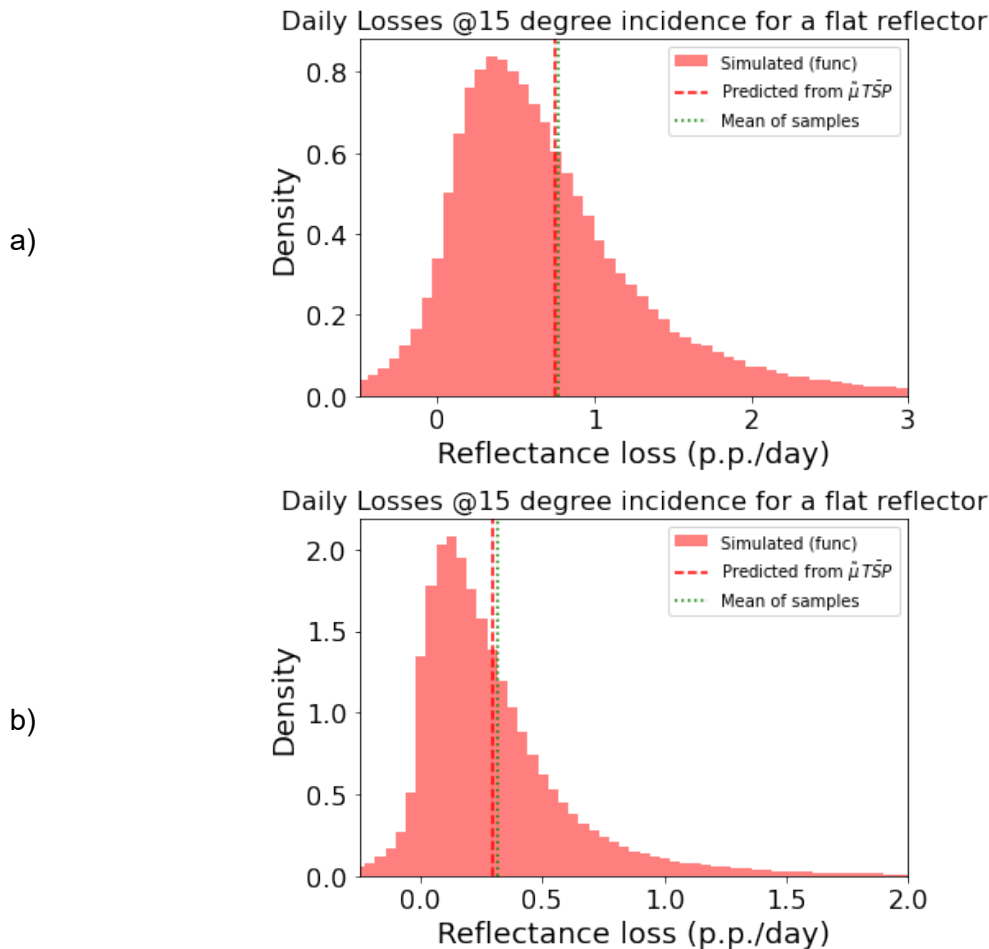


Figure 4. Wodonga – Monthly Average PM_x (left) ; Intra-day synchronously averaged PM_x ratio (right). Missing data are due to maintenance of the device from June to August 2022

4. Results

The stochastic soiling model discussed in Sections 2.1 and 2.2 is applied in this study on the available datasets of airborne dust concentration (either expressed in terms of TSP or PM10, depending on the deployed dust sampler) to assess the expected daily losses for each site. In Figure 5, the statistical distribution of expected reflectance losses for a horizontal mirror is shown for the three sites. The estimated reflectance daily losses for the site in Brisbane have a mean of 0.77 pp/day, a median of 0.56 pp/day, and a strong positive skewness. The significant width of the distribution suggests that most reflectance daily losses happen in the interval 0.26 pp/day to 1.00 pp/day. The expected "worst case scenario" at the 97.5th percentile corresponds to a loss of 2.88 pp/day. The estimated reflectance daily losses for the site in Mount Isa have a mean of 0.31 pp/day, a median of 0.22 pp/day, and an only slight positive skewness. The width of the distribution is limited suggesting that most reflectance daily losses happen between 0.09 pp/day and 0.41 pp/day. The expected "worst case scenario" at the 97.5th percentile corresponds to a loss of 1.28 pp/day. The estimated reflectance daily losses for the site in Wodonga have a mean of 0.72 pp/day, a median of 0.58 pp/day, and a significant positive skewness. The width of the distribution suggests that most reflectance daily losses happen in the interval 0.37 pp/day to 0.87 pp/day. The width of the distribution suggests that most reflectance daily losses happen in the interval between 0.37 pp/day and 0.87 pp/day. The expected "worst case scenario" at the 97.5th percentile corresponds to a loss of 1.99 pp/day. It is noteworthy to observe the higher expected reflectance losses for the urban environment at 0.77 pp/day (a) and the rural environment at 0.72 pp/day (c) with respect to the very low losses in the outback location at 0.31 pp/day (b).



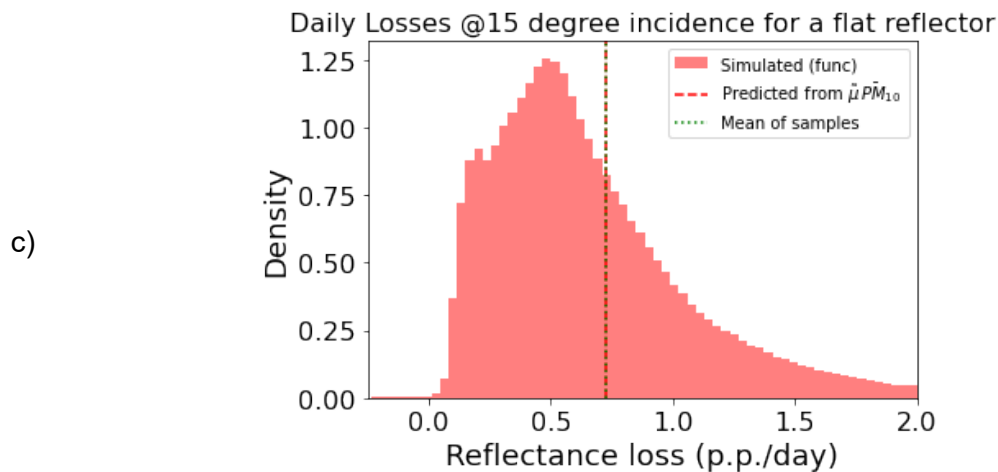


Figure 5. Probability density functions of soiling losses for the three sites: a) Brisbane, b) Mount Isa, c) Wodonga

5. Conclusions

Probability distributions of daily reflectance losses have been estimated for three Australian sites based on extended datasets of measured airborne dust concentration. The results show that the knowledge of dust concentration at prospective CSP plant locations for an extended amount of time (at least one year) could provide reliable assessment of expected reflectance losses for heliostats deployed on site. The analysis presented in this study represents a first-of-its-kind for CSP soiling-induced reflectance losses. The information provided by the histograms in Figure 5 are of paramount importance for CSP owners and operators, since it enables proper planning of mitigation activities with respect to heliostats soiling. Furthermore, when an exploratory experimental campaign is conducted on a potential CSP site, the shown graphs become a powerful tool for assessing expected losses, project de-risking and as a performance index for site selection.

Data availability statement

The data for all experimental campaigns, model inputs, and model parameter values can also be found in the GitHub repository (https://github.com/cholette/mirror_soiling_data).

Author contributions

Giovanni Picotti: Writing – original draft, Methodology, Investigation, Conceptualization, Data curation. **Huy Truong-Ba:** Writing – review & editing, Visualization, Data curation. **Cody B. Anderson:** Writing – review & editing, Visualization, Data curation. **Michael E. Cholette:** Writing – review & editing, Methodology, Formal Analysis, Supervision, Project administration, Funding acquisition, Conceptualization. **Theodore A. Steinberg:** Supervision, Project administration, Funding acquisition. **Bruce Leslie:** Writing – review & editing, Resources, Project administration.

Competing interests

The authors declare that they have no competing interests.

Underlying and related material

The models exploited in this study were implemented in Python and are now available in the HelioSoil GitHub repository (<https://github.com/cholette/HelioSoil>).

Funding

G. Picotti, C.B. Anderson, M.E. Cholette and T.A. Steinberg acknowledge the support of the Australian Government for this study, through ARENA within the framework of ASTRI (Project ID P54). The same authors also acknowledge the support of the U.S. Department of Energy's Solar Energy Technologies Office via the Soiling Subtask of the Heliostat Consortium (HelioCon).

Acknowledgement

The authors would like to also acknowledge the support of Vast leadership (especially Kurt Drewes and Bruce Leslie), and Paul Matuschka from Mars Petcare.

References

- [1] C. B. Anderson, G. Picotti, M. E. Cholette, B. Leslie, T. A. Steinberg, and G. Manzoloni, "Heliostat-field soiling predictions and cleaning resource optimization for solar tower plants," *Appl. Energy*, vol. 352, p. 121963, Dec. 2023, doi: 10.1016/j.apenergy.2023.121963.
- [2] G. Zhu *et al.*, "Roadmap to Advance Heliostat Technologies for Concentrating Solar-Thermal Power," NREL/TP-5700-83041, Sep. 2022. doi: 10.2172/1888029.
- [3] M. Mehos *et al.*, "Concentrating Solar Power Best Practices Study," NREL/TP--5500-75763, 1665767, MainId:7049, Jun. 2020. doi: 10.2172/1665767.
- [4] G. Picotti *et al.*, "Optimization of cleaning strategies for heliostat fields in solar tower plants," *Sol. Energy*, vol. 204, pp. 501–514, Jul. 2020, doi: 10.1016/j.solener.2020.04.032.
- [5] G. Picotti, M. E. Cholette, F. Casella, M. Binotti, T. A. Steinberg, and G. Manzoloni, "Dynamic thermal analysis of an external cylindrical receiver in an object-oriented modelling paradigm," presented at the SOLARPACES 2020: 26th International Conference on Concentrating Solar Power and Chemical Energy Systems, 2022. doi: 10.1063/5.0085650.
- [6] G. Picotti, P. Borghesani, G. Manzoloni, M. E. Cholette, and R. Wang, "Development and experimental validation of a physical model for the soiling of mirrors for CSP industry applications," *Sol. Energy*, vol. 173, pp. 1287–1305, Oct. 2018, doi: 10.1016/j.solener.2018.08.066.
- [7] J. Ballestrín *et al.*, "Soiling forecasting of solar plants: A combined heuristic approach and autoregressive model," *Energy*, vol. 239, p. 122442, Jan. 2022, doi: 10.1016/j.energy.2021.122442.
- [8] W. Javed, B. Guo, and B. Figgis, "Modeling of photovoltaic soiling loss as a function of environmental variables," *Sol. Energy*, vol. 157, pp. 397–407, Nov. 2017, doi: 10.1016/j.solener.2017.08.046.
- [9] F. Terhag, F. Wolfertstetter, S. Wilbert, T. Hirsch, and O. Schaudt, "Optimization of cleaning strategies based on ANN algorithms assessing the benefit of soiling rate forecasts," presented at the SOLARPACES 2018: International Conference on Concentrating Solar Power and Chemical Energy Systems, Casablanca, Morocco, 2019, p. 220005. doi: 10.1063/1.5117764.

- [10] A. M. Bonanos, M. J. Blanco, and K. Milidonis, "Characterization of mirror soiling in CSP applications," presented at the SOLARPACES 2019: International Conference on Concentrating Solar Power and Chemical Energy Systems, Daegu, South Korea, 2020, p. 030007. doi: 10.1063/5.0028528.
- [11] A. Heimsath *et al.*, "Automated monitoring of soiling with AVUS instrument for improved solar site assessment," presented at the SolarPACES 2017: International Conference on Concentrating Solar Power and Chemical Energy Systems, Santiago, Chile, 2018, p. 190008. doi: 10.1063/1.5067193.
- [12] R. Conceição, H. G. Silva, and M. Collares-Pereira, "CSP mirror soiling characterization and modeling," *Sol. Energy Mater. Sol. Cells*, vol. 185, pp. 233–239, Oct. 2018, doi: 10.1016/j.solmat.2018.05.035.
- [13] G. Picotti, M. E. Cholette, C. B. Anderson, T. A. Steinberg, and G. Manzoloni, "Stochastic soiling loss models for heliostats in Concentrating Solar Power plants," *Sol. Energy*, vol. 263, no. 111945, 2023.
- [14] J. H. Seinfeld and S. N. Pandis, *Atmospheric chemistry and physics: from air pollution to climate change*. New York: Wiley-Interscience, 1998.